

# Myoglobin and Hemoglobin Rotational Diffusion in the Cell

Dong Wang, Ulrike Kreutzer, Youngran Chung, and Thomas Jue

Biological Chemistry Department, University of California Davis, Davis, California 95616-8635 USA

**ABSTRACT** The detection of the  $^1\text{H}$  NMR signal of myoglobin (Mb) in tissue opens an opportunity to examine its cellular diffusion property, which is central to its purported role in facilitating oxygen transport. In perfused myocardium the field-dependent transverse relaxation analysis of the deoxy Mb proximal histidyl  $\text{N}_\delta\text{H}$  indicates that the Mb rotational correlation time in the cell is only  $\sim 1.4$  times longer than it is in solution. Such a mobility is consistent with the theory that Mb facilitates oxygen diffusion from the sarcoplasm to the mitochondria. The microviscosities of the erythrocyte and myocyte environment are different. The hemoglobin (Hb) rotational correlation time is 2.2 longer in the cell than in solution. Because both the overlapping Hb and Mb signals are visible *in vivo*, a relaxation-based NMR strategy has been developed to discriminate between them.

## INTRODUCTION

Myoglobin has served as a key model in the study of the rules governing the protein structure-function relationship. Tons of biophysical data have pinpointed the various molecular interactions that alter the oxygen binding kinetics (Antonini and Brunori, 1971). At the same time, crystallographic NMR analyses have detailed the three-dimensional structure in various ligation and oxidation states (Takano, 1977a,b; Phillips, 1980; Dalvit and Wright, 1987; Mabbitt and Wright, 1985; La Mar et al., 1993; Busse and Jue, 1994). Yet the abundance of experimental data has not definitively established the Mb function in the cell.

In the conventional view, Mb is an oxygen storage protein and can facilitate oxygen diffusion from the sarcoplasm to the mitochondria. The facilitated diffusion hypothesis is predicated on the contrast between the oxygen-carrying capacity of Mb versus the low solubility of free oxygen in the cell (Wittenberg, 1970; Wittenberg and Wittenberg, 1989; Conley and Jones, 1996). Under certain conditions, oxygen diffuses more rapidly through a heme protein solution than through a heme-free solution. Although a substantial body of *in vitro* experimental and theoretical evidence supports the proposed model, the critical Mb diffusion constant in the cell is still undetermined (Riveros-Moreno and Wittenberg, 1972; Jurgens et al., 1994; Papadopoulos et al., 1995). Indeed, if the Mb translational diffusion is much slower than the free diffusion of oxygen, then Mb cannot compete effectively to meet respiratory demands. The model must then overcome a very serious challenge.

Critical to the facilitated diffusion model is an accurate determination of myoglobin diffusion in the cell. Such measurements must overcome formidable experimental hurdles (Papadopoulos et al., 1995; Riveros-Moreno and Wittenberg, 1972; Jurgens et al., 1994). Recently  $^1\text{H}$  NMR meth-

odology has opened an opportunity to examine directly the physical properties of cellular Mb. In a Langendorff perfused heart model, investigators have demonstrated that the signals from the deoxy-Mb proximal histidyl  $\text{N}_\delta\text{H}$  and the oxy-Mb Val E11  $\gamma\text{CH}_3$  are detectable, are completely NMR visible, originate only from the cell, and can quantitatively reflect the cellular response to a wide range of oxygen levels (Kreutzer and Jue, 1991; Kreutzer et al., 1992). With a localized Mb proximal histidyl  $\text{N}_\delta\text{H}$  signal, researchers can now confidently utilize the paramagnetic relaxation theory to examine Mb rotational diffusion in the cell and to assess whether the results are consistent with Mb's hypothesized role in facilitating oxygen transport (Gueron, 1975; Vega and Fiat, 1976; Livingston et al., 1983).

The field-dependent relaxation analysis of the proximal histidyl  $\text{N}_\delta\text{H}$  signal yields a Mb rotational correlation time in the cell only 1.4 times slower than it is in solution. Such a rapid correlation time is consistent with the postulated Mb role in facilitating oxygen diffusion. Similarly, the erythrocyte environment increases the Hb rotational diffusion 2.2 times. Because the Mb and Hb relaxation properties in their respective cellular environments are sufficiently different, relaxation-based spectral editing techniques can discriminate these signals in blood perfused tissue and form a basis for further exploration of the properties and function of Mb *in vivo*.

## MATERIALS AND METHODS

### Myoglobin

Myoglobin solutions were prepared directly from lyophilized horse heart protein (Sigma). Preparation of deoxy-Mb and MbCO followed the previously described procedures (Kreutzer et al., 1993).

In perfused myocardium studies, male Sprague-Dawley rats (350–400 g) were first anesthetized by an intraperitoneal injection of sodium pentobarbital (60 mg/kg) and heparinized (1000 U/kg) by injection into the femoral vein. The hearts were isolated and perfused by a modified Langendorff technique at  $25^\circ\text{C}$  (Kreutzer and Jue, 1995; Chung and Jue, 1996). A peristaltic pump (Rainin Rabbit) controlled the perfusion rate. A saline-filled latex balloon inserted into the left ventricle monitored the heart rate (HR) and left ventricular pressure (LVP) via a strain gauge transducer

Received for publication 23 May 1997 and in final form 4 August 1997.

Address reprint requests to Dr. Thomas Jue, Department of Biological Chemistry, University of California–Davis, Davis, CA 95616-8635. Tel.: 916-752-4569; Fax: 916-752-3516; E-mail: tjue@ucdavis.edu.

© 1997 by the Biophysical Society

0006-3495/97/11/2764/07 \$2.00

(Statham P23XL) connected to an oscillographic recorder (Gould RS 3200). The balloon volume was adjusted to give an end-diastolic pressure of 5–7 mm Hg. The typical rate pressure product, calculated from HR times the left ventricular developed pressure (LVDP), was  $14.2 \pm 2.6 \times 10^3 \text{ s}^{-1} \text{ mm Hg}$ .

## Hemoglobin

Blood cell samples were prepared directly from freshly outdated whole blood without further purification (Sacramento Blood Bank). For deoxy Hb, the sample was first gently flushed with nitrogen gas before it was transferred to an NMR tube. A slight stoichiometric excess of sodium dithionite was injected into the anaerobically sealed NMR tube. The red blood cells do not exhibit any increased lysing, and the cellular Hb signals do not display any spectral perturbation, when compared to Hb signals obtained after simple nitrogen degassing (Kreutzer et al., 1993). The sample then settled to about a 1:1 ratio of cell to plasma before the NMR spectral acquisition began. After the NMR experiment, sample centrifugation separated the plasma component, which contained a negligible amount of lysed Hb, as determined by optical spectral analysis (HP 8452A) of the  $\alpha$  and  $\beta$  bands of HbO<sub>2</sub> at 542 and 576 nm. Further analysis of the lysate indicated that the Hb content contained an insignificant amount of metHb.

The hemoglobin solution preparation followed previously reported procedures (Antonini and Brunori, 1971; Kreutzer et al., 1993). The blood was centrifuged (10 min,  $600 \times g$ ) and washed three times with 1% NaCl solution at 4°C. Approximately 3 volumes of distilled H<sub>2</sub>O was used to lyse the erythrocytes. Centrifugation (30 min,  $30,000 \times g$ ) removed the cell debris. The lysate was then dialyzed against 100 mM potassium phosphate buffer at pH 7.4. Ultrafiltration with an Amicon cell first concentrated the solution and then, if necessary, permitted the H<sub>2</sub>O/D<sub>2</sub>O exchange with 99.8% D<sub>2</sub>O (Cambridge Isotope Laboratories, Woburn, MA), typically 1/5 v/v. A slight stoichiometric excess of sodium dithionite was added to a degassed Hb solution to form deoxy-Hb. Carbon monoxide was added to oxy-Hb to form HbCO.

## NMR

Erythrocyte and protein spectra were acquired at different magnetic fields (2, 4.7, 7, 8.4, 9.2, and 11.5T), with GE CSI 2T, Nicolet 200, Nicolet 360, GE Omega 300, Bruker 400, and GE Omega 500 spectrometers. A 1331 pulse sequence was used to suppress the water signal. Depending on the signal-to-noise requirement, the number of scans varied between 1,000 and 10,000. Exponential filtering improved the final signal-to-noise. The <sup>1</sup>H signals were referenced to the water line, 4.76 ppm at 25°C, which in turn was calibrated against 2,2-dimethyl-2-silapentane-5-sulfonate acid. A Hahn spin-echo pulse sequence was used to measure the  $T_2$  relaxation. The  $T_1$  relaxation measurements of deoxy-Hb and Mb employed both inversion recovery and saturation recovery sequences. The  $\tau$  values ranged from 20  $\mu$ s to 300 ms.

Sigmaplot software (Jandel Scientific) was used to analyze the  $T_1$  and  $T_2$  relaxation data. For the  $T_2$  relaxation, the curve fitting used a single exponential decay. The water linewidth was subtracted from the proximal histidyl N<sub>8</sub>H signal to remove the field inhomogeneity contribution. Line-width analysis then utilized either Omega 6.2, UXNMR, or the Sigmaplot curve fit algorithms. A three-parameter fit was used to analyze the  $T_1$  data.

## Analysis of rotational diffusion

The paramagnetic relaxation theory of Gueron and Vega indicates that the field-dependent transverse relaxation of a paramagnetic molecule can be

described by the equation

$$\frac{1}{T_2} = \frac{4}{5} \frac{\gamma^2 g^4 \beta^4 S^2 (S+1)^2 B_o^2 \tau_r}{9 r^6 k^2 T^2} + \frac{7}{15} \left( \frac{\gamma^2 g^2 \beta^2}{r^6} \right) S(S+1) T_{1e} + \frac{1}{T_2^{\text{dia}}} \quad (1)$$

where  $\gamma_1$  = proton magnetogyric ratio =  $26.7519 \times 10^3 \text{ rad gauss}^{-1} \text{ s}^{-1}$ ;  $g$  =  $g$  factor;  $\beta$  = Bohr magneton =  $9.27 \times 10^{-21} \text{ erg/gauss}$ ;  $S$  = spin number;  $\tau_r$  = rotational correlation time;  $T_{1e}$  = electron spin lattice relaxation time;  $T_2^{\text{dia}}$  = diamagnetic spin-spin relaxation time;  $B_o$  = magnetic field;  $r$  = the internuclear distance between the heme iron and the proximal histidyl N<sub>8</sub>H proton = 5.17 Å for Mb and 5.15 Å for Hb;  $T$  = temperature in Kelvin = 293 K;  $k$  = Boltzmann constant =  $1.38 \times 10^{-16} \text{ erg K}^{-1}$  (Gueron, 1975; Vega and Fiat, 1976).

The equation states that a field-dependent graphical analysis of transverse relaxation versus  $(B_o)^2$  will yield the  $\tau_r$  from the slope and the  $T_{1e}$  from the intercept. Subtracting the diamagnetic contribution, as reflected in the corresponding signal of the Val E11 signal, leads to the linewidths of the Mb and Hb proximal histidyl N<sub>8</sub>H signals that will reflect the dominant paramagnetic  $T_2$  relaxation (Johnson et al., 1977; Livingston et al., 1983). The Stokes-Einstein equation for rotational diffusion

$$\tau_r = \frac{4\pi r^3 \eta}{kT} \quad (2)$$

where  $r$  is the molecular radius,  $\eta$  is the solvent viscosity,  $k$  is Boltzmann's constant, and  $T$  is the temperature in Kelvins, provides then a theoretical basis to compare the NMR determined  $\tau_r$  against values obtained from other physical methods (Everhart et al., 1982; Marshall et al., 1983).

## RESULTS

Fig. 1 shows the 300-MHz <sup>1</sup>H NMR spectra of deoxy-Hb in solution and in erythrocytes. The characteristic hyperfine shifted signals between 30 and 10 ppm are shown in Fig. 1 A, and the erythrocyte Hb spectrum appears in Fig. 1 B. Except for additional broadening, the two spectral features

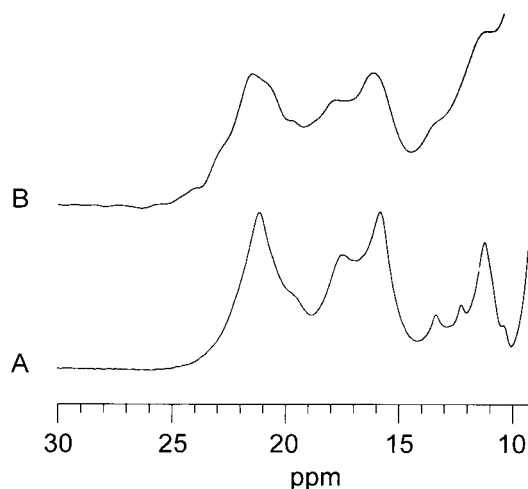


FIGURE 1 <sup>1</sup>H NMR 300 MHz spectra of deoxy-Hb in solution and in erythrocytes at 25°C. The spectral region between 30 and 10 ppm is shown for (A) deoxy-Hb in solution and (B) deoxy-Hb in erythrocyte.

are closely matched and confirm that cellular Hb signals are detectable.

The solution Mb and Hb proximal histidyl N<sub>δ</sub>H signals are shown in Fig. 2. Fig. 2 A displays the spectrum of the proximal histidyl N<sub>δ</sub>H from Mb; Fig. 2 B displays the spectrum from Hb. The Mb signal appears at 79 ppm at 25°C and exhibits a linewidth of 235 Hz. The spectrum from Hb also shows the corresponding proximal histidyl N<sub>δ</sub>H signals at 64 and 76 ppm from the  $\alpha$ - and  $\beta$ -subunits (Takahashi et al., 1980; La Mar et al., 1977, 1980; Ho and Russu, 1981). The Hb signal linewidth of the  $\beta$  proximal histidyl N<sub>δ</sub>H is 935 Hz.

In tissue, the corresponding Mb and Hb proximal histidyl N<sub>δ</sub>H signals are shown in Fig. 3. The Mb proximal histidyl N<sub>δ</sub>H signal from the myocardium resonates at the same chemical shift as the solution state signal (Fig. 3 A). The linewidth has increased to 385 Hz. Fig. 3 B shows the Hb proximal histidyl N<sub>δ</sub>H signals. These signals appear in the baseline uncorrected spectra at 64 and 76 ppm at 25°C (Ho and Russu, 1981; Kreutzer et al., 1993). The chemical shift position and intensity of the  $\alpha$  proximal histidyl N<sub>δ</sub>H signal in the figure are distorted by the baseline correction algorithm and the pulse excitation profile, which is centered at 76 ppm (Kreutzer et al., 1993; Fetler et al., 1995). The linewidth  $\beta$  proximal histidyl N<sub>δ</sub>H is 1325 Hz.

The field-dependent analysis of the transverse relaxation of the Hb and Mb proximal histidyl N<sub>δ</sub>H linewidth versus ( $B_0$ )<sup>2</sup> in solution and in the cell is shown in Fig. 4 (Johnson et al., 1977). For Mb the ratio of the two slopes is 1.4.

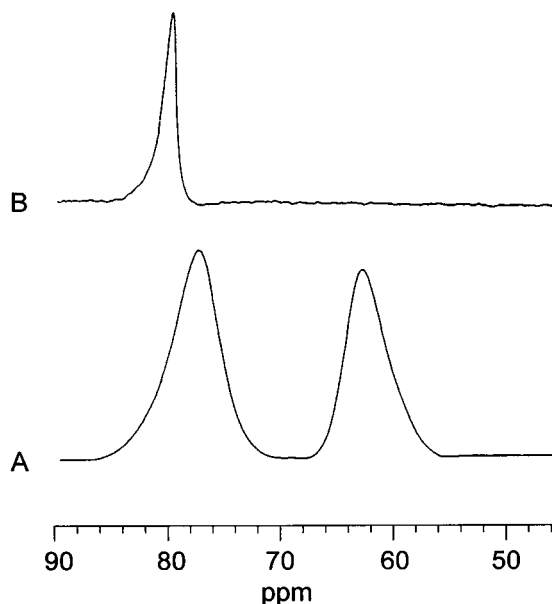


FIGURE 2 <sup>1</sup>H NMR 300 MHz spectra of the proximal histidyl N<sub>δ</sub>H signals of deoxy-Mb and deoxy-Hb in solution at 25°C. (A) The deoxy-Hb spectrum exhibits the characteristic 64 and 76 ppm signals, corresponding to the  $\alpha$ - and  $\beta$ -subunits. (B) The deoxy-Mb spectrum shows a signal at 79 ppm. The slight distortion in the  $\alpha$ -subunit peak's chemical shift position and intensity arises from baseline correction.

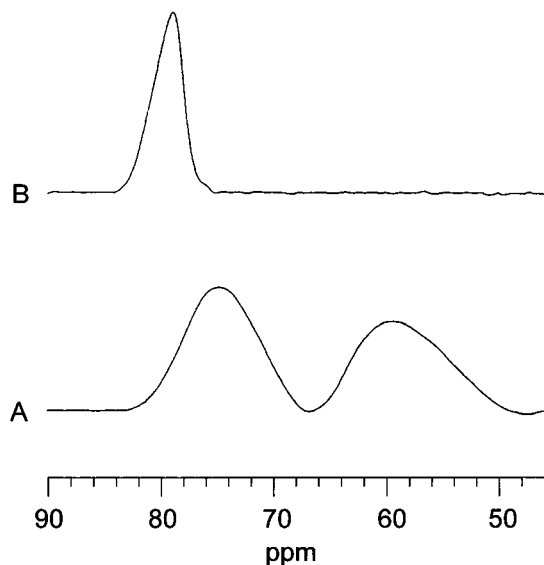


FIGURE 3 <sup>1</sup>H NMR 300 MHz spectra of deoxy-Hb in erythrocyte and in myocardium at 25°C. (A) From the baseline uncorrected spectra, the deoxy-Hb spectrum displays the proximal histidyl N<sub>δ</sub>H signals from the  $\beta$ - and  $\alpha$ -subunits at 76 and 64 ppm, respectively. The polynomial baseline algorithm distorts the chemical shift and intensity of the  $\alpha$ -subunit peak, which is excited by a binomial pulse with a maximum centered at 76 ppm. (B) The corresponding signal from deoxy-Mb in myocardium appears at 79 ppm.

Evaluating Eq. 1 with the appropriate physical constants yields a rotational correlation of  $9.7 \pm 0.3 \times 10^{-9}$  s and  $13.6 \pm 1.3 \times 10^{-9}$  s for solution and tissue Mb, respectively (Fig. 4 A) (Gueron, 1975; Vega and Fiat, 1976). For Hb the ratio of the two slopes is 2.2 (Fig. 4 B), yielding a correlation time  $37.7 \pm 2.1 \times 10^{-9}$  s and  $84 \pm 4.3 \times 10^{-9}$  s for erythrocytes and solution Hb, respectively. The  $T_{1e}$  is  $7.5 \pm 3.2 \times 10^{-12}$  s and  $6.5 \pm 3.6 \times 10^{-12}$  s. The intercepts yield a  $T_{1e}$  of  $2.6 \pm 0.4 \times 10^{-12}$  s and  $3.0 \pm 1.4 \times 10^{-12}$  s, respectively. Both the Mb and Hb rotational correlation time and  $T_{1e}$  values are tabulated in Table 1.

At 300 MHz the solution Mb and Hb proximal histidyl N<sub>δ</sub>H  $T_2$  values are 530  $\mu$ s and < 190  $\mu$ s (Fetler et al., 1995). The corresponding  $T_1$  values are  $12.2 \pm 0.5$  ms and  $9.1 \pm 0.4$  ms, respectively. Erythrocyte Hb yields a  $T_1$  of ~5–6 ms, whereas cellular Mb has insufficient signal-to-noise for a relaxation measurement. The  $T_2$  contrast is enhanced in vivo, because cellular Mb has a rotational correlation time only slightly longer than in solution, whereas the Hb correlation time is much longer. Fig. 5 A displays the <sup>1</sup>H spectra of 0.1 mM deoxy-Mb solution dissolved in deoxygenated erythrocytes. The two proximal histidyl N<sub>δ</sub>H signals of Hb dominate the spectrum, with only a slight hint of the corresponding Mb peak at 79 ppm. A 1-ms spin-echo pulse sequence readily suppresses the Hb signal and edits the Mb signal (Fig. 5 B). A similar discrimination is observed in the corresponding Val E11 signals (data not shown).

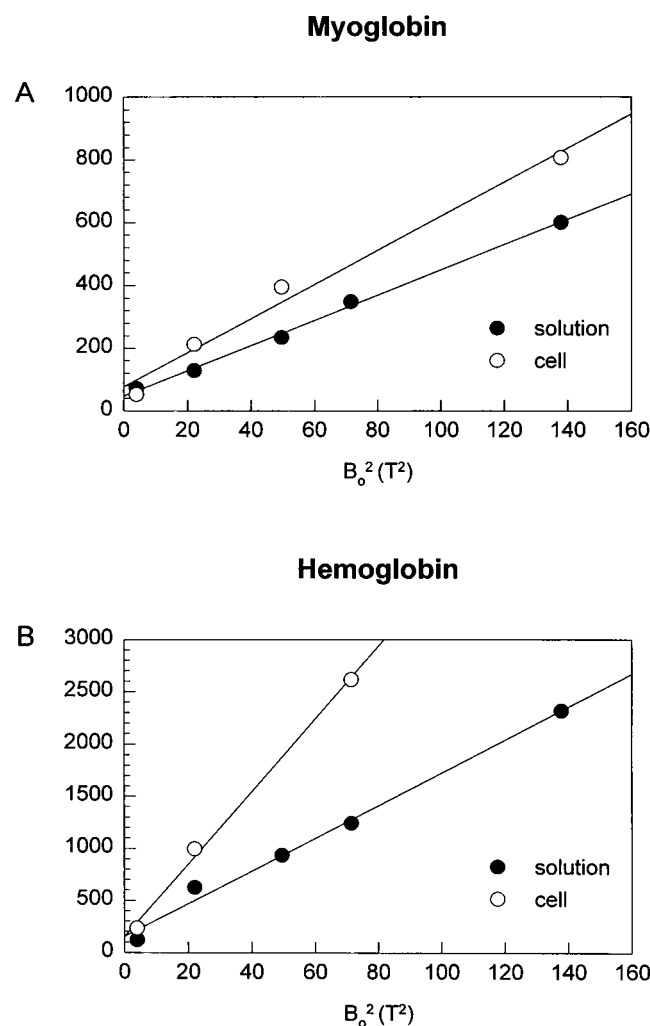


FIGURE 4 Field-dependent plot of linewidth versus square of the magnetic field ( $B_0$ )<sup>2</sup> for Mb and Hb. (A) Field-dependent analysis of deoxy-Mb proximal histidyl  $N_\delta H$  signal in solution and in the myocardium. (B) Field-dependent analysis of deoxy-Hb  $\beta$  proximal histidyl  $N_\delta H$  signal in solution and in erythrocyte.

## DISCUSSION

### Visibility of cellular Mb and Hb signals

Recently investigators have failed to observe the  $^1H$  NMR deoxy-Hb signal of the proximal histidyl  $N_\delta H$  in erythrocytes and have suggested that the cellular microviscosity

TABLE 1 Rotational correlation time and  $T_{1\rho}$  of Mb and Hb

	Slope	$\tau_r \times 10^9$ s	$r$	$\Delta\nu^0$	$\Delta\nu^{dia}$	$\Delta\nu^0 - \Delta\nu^{dia}$	$T_{1\rho} \times 10^{12}$ s
Mb (s)	4.0	$9.7 \pm 0.3$	0.99	47	11	36	$2.6 \pm 0.4$
Mb (cell)	5.6	$13.6 \pm 1.3$	0.98	71	30	41	$3.0 \pm 1.4$
Hb (s)	15.7	$37.7 \pm 2.1$	0.99	151	44	107	$7.5 \pm 3.2$
Hb (cell)	35.0	$84.0 \pm 4.3$	0.99	150	60	90	$6.5 \pm 3.6$

The  $\Delta\nu^{dia}$  for solution Mb and Hb was taken from the respective MbO<sub>2</sub> Val E11 linewidths: for Mb/Hb in solution, 11 and 44 Hz; for Mb and Hb in cell, 30 and 60 Hz, respectively.  $r$  = linear regression correlation coefficient. Error is  $\pm$  standard error.

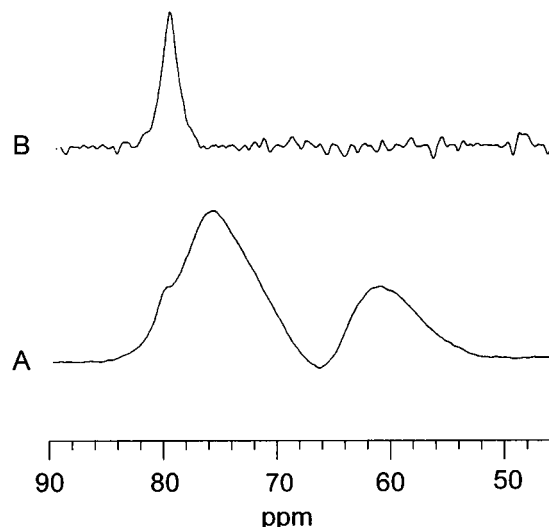


FIGURE 5  $^1H$  NMR 300 MHz spectra of 0.1 mM deoxy-Mb dissolved in physiological saline solution mixed with erythrocytes at 25°C. (A) Upon deoxygenation of both Mb and erythrocyte Hb, the Hb proximal histidyl  $N_\delta H$  signals from the  $\alpha$ - and  $\beta$ -subunits dominate the spectrum. Only a hint of the deoxy-Mb signal appears at 79 ppm. (B) A 1-ms spin echo suppresses the erythrocyte Hb signal and selects only the Mb proximal histidyl  $N_\delta H$  peak.

impedes molecular mobility, which then leads to severe broadening of the Hb signal beyond detection (Wang et al., 1993). That observation appears to be inconsistent with previously published reports (London et al., 1975; Ho and Russu, 1981; Everhart and Johnson, 1982; Livingston et al., 1983; Kuchel and Chapman, 1991; Kreutzer et al., 1993; Fetter et al., 1995). Figs. 1 and 3 clearly indicate that the cellular deoxy-Hb signals are indeed visible and match the corresponding solution spectra.

Even though the spectral features are identical, the erythrocyte Hb proximal histidyl  $N_\delta H$  signals are broadened, which can reflect either chemical exchange or enhanced microviscosity. However, solution measurements indicate that the  $N_\delta H$  paramagnetic relaxation rate at physiological pH is much more rapid than its exchange rate with bulk water (La Mar et al., 1981). For Hb the exchange half-life is on the order of hours, consistent with an amino acid residue buried in the heme pocket (Jue et al., 1984). Any linewidth broadening arising from water-NH exchange is then insignificant.

Given this view, other chemical exchange processes would also not contribute significantly, because the reaction time must be much faster than the  $T_2$  relaxation times of  $<190 \mu s$ —a time scale that is not commonly affected by chemical exchange dynamics. It would be consistent to posit that the signal line broadening observed in the cellular environment arises from an enhanced microviscosity.

A similar argument is applicable in the analysis of the Mb signal (La Mar et al., 1981). Moreover, the cellular Mb signal reflects a totally NMR visible and mobile pool in the cell, because the biochemical and NMR determinations of

tissue Mb are in excellent agreement (Kreutzer and Jue, 1991).

### Mb and Hb rotational diffusion in solution

The contrast in microviscosity is manifested in the distinct rotational correlation times. The proximal histidyl N<sub>δ</sub>H signals of both Mb and Hb exhibit a field-dependent transverse relaxation that leads to a determination of the rotational correlation time and the  $T_{1e}$ , as specified in Eq. 1 (Gueron, 1975; Vega and Fiat, 1976). Researchers have already detected such field-dependent relaxation in the hyperfine shifted resonances between 30 and 15 ppm of deoxy-Mb and Hb solution spectra (Johnson et al., 1977).

However, the peaks in the 30–15 ppm spectral region are composite in nature and require careful deconvolution to accurately separate the overlapping components, especially at low fields (Viggiano et al., 1979). Unlike the deoxy-Mb and Hb signals in the 30–15 ppm region, the proximal histidyl N<sub>δ</sub>H signals have no spectral interference around 79 ppm. Field-dependent relaxation analysis of the deoxy-Mb and Hb proximal histidyl N<sub>δ</sub>H resonances yields correlation times of  $9.7 \pm 0.3 \times 10^{-9}$  s and  $37.7 \pm 1.3 \times 10^{-9}$  s at 25°C. The values are consistent with the Stokes-Einstein equation prediction of  $11 \times 10^{-9}$  s and  $44 \times 10^{-9}$  s at 10°C and with other experimental determinations, as tabulated in Table 2. Moreover, the Hb/Mb  $\tau_r$  ratio of 3.9 is in excellent agreement with the value predicted from the Stokes-Einstein equation as the molecular volume of globular proteins scales up from a monomeric to a tetrameric form. No Hb fluctuation in the heme pocket is apparent, which would give rise to a Hb/Mb  $\tau_r$  ratio of 1.4, as detected in perturbed angular correlation studies (Marshall et al., 1980, 1983).

### Mb and Hb rotational diffusion in the cell

According to the generally accepted biochemical view, Mb stores oxygen or facilitates oxygen diffusion from the sarcoplasm to the mitochondria (Wittenberg, 1970). Implicit in

the facilitated diffusion model is a critical requirement for a sufficiently mobile Mb molecule to compete effectively with simple oxygen diffusion. So far, confirming a rapid Mb diffusion in tissue has posed a major experimental challenge (Riveros-Moreno and Wittenberg, 1972; Jurgens et al., 1994; Papadopoulos et al., 1995).

An indirect observation of myoglobin's cellular mobility is available through the analysis of its rotational correlation time. Researchers have already utilized the proximal histidyl N<sub>δ</sub>H resonances to determine the Mb  $\tau_r$  in excised heart tissue (Livingston et al., 1983). However, the unphysiological muscle preparation, the potential contribution from extracellular Mb released from necrotic tissue, and the two point linear analysis of field-dependent relaxation data have raised questions about the accuracy of the determined *in vivo* value. The present study has utilized a standard physiological heart model, which does not contain any Mb contribution from the extracellular space, and has secured data from several magnetic fields (Kreutzer and Jue, 1991). The field-dependent relaxation analysis of Mb in viable heart tissue yields a cellular correlation time of  $13.6 \pm 1.3 \times 10^{-9}$  s at 25°C. The ratio of the myocyte Mb/solution Mb correlation time is then a factor of 1.4, far lower than the 2.3 factor noted in the earlier study (Livingston et al., 1983). For Hb, the erythrocyte correlation time is  $84 \pm 4.3 \times 10^{-9}$  s, and the ratio of erythrocyte Hb/solution Hb correlation time is a factor of 2.2.

The increase in the Mb  $\tau_r$  of 1.4 times is consistent with a relatively mobile molecule in the cellular environment and presumably originates from the increased cellular microviscosity. Given that the overall viscosity of dilute Mb solution is 1.1 centipoise, the cellular microviscosity is then  $\sim 1.5$  centipoise, a number that is consistent with previous findings and with a fluid cellular environment (London et al., 1975; Livingston et al., 1983). Furthermore, if the molecular hydrodynamics in solution and in the cell are similar and if unrestricted diffusion exists, then the estimated Mb translational diffusion constant in solution,  $6\text{--}8 \times 10^{-7}$  cm<sup>2</sup>/s, is only slightly smaller in the cell,  $4\text{--}6 \times 10^{-7}$  cm<sup>2</sup>/s (Wit-

**TABLE 2** Comparison of Mb/Hb  $\tau_r$  and  $T_{1e}$  of Mb and Hb with other experimental results

Method	$\tau_r \times 10^9$ s	$\tau_r \times 10^9$ s	$T_{1e} \times 10^{12}$ s	$T_{1e} \times 10^{12}$ s	°C	Reference
	Mb solution	Hb solution	Mb solution	Hb solution		
Stokes-Einstein	11	44			10	
NMR	9.7	37.7	2.6	7.5	25	This work
NMR	5–6	25	6.1	6.1	30	1
NMR	6.4					2
Perturbed angular correlation	16	23			10	3
Fluorescence	8.3–9.6	14.5			20–25	4
	$\tau_r \times 10^9$ s	$\tau_r \times 10^9$ s	$T_{1e} \times 10^{12}$ s	$T_{1e} \times 10^{12}$ s	°C	
	Mb cell	Hb cell	Mb cell	Hb cell		
NMR	13.6	56.0	3.0	6.5	25	This work
NMR	14.7				13	2

1. Johnson et al. (1977).

2. Livingston et al. (1983).

3. Marshall et al. (1980, 1983).

4. Yguerabide et al. (1970); Stryer (1965).

tenberg, 1970). It would imply that with a  $pO_2$  of 10 torr at the cell boundary, Mb-facilitated diffusion will account for ~50% of the oxygen flux. In contrast, microinjection studies have determined diffusion constants of  $2.0\text{--}2.9 \times 10^{-7} \text{ cm}^2/\text{s}$ , which would ascribe only 25% of the total  $O_2$  flux to Mb-mediated transport (Papadopoulos et al., 1995). Definitive experimental measurement of the Mb translational diffusion in the cell is still required to firmly establish the Mb role in facilitating oxygen diffusion.

For Hb, the shift from solution to cell state entails an increase in  $\tau_r$  of 2.2 times. That shift is consistent with a higher microviscosity in erythrocyte than in myocyte. The interpretation is consonant with the observation from  $^{13}\text{C}$  relaxation and translational diffusion measurements (London et al., 1975; Kuchel and Chapman, 1991).

### Electronic properties of cellular Mb and Hb

The field-dependent paramagnetic relaxation analysis yields insight into the electronic structure of Mb and Hb in the solution and in the cell. For Mb the respective  $T_{1e}$  values are  $2.6 \pm 0.4 \times 10^{-12} \text{ s}$  and  $3.0 \pm 1.4 \times 10^{-12} \text{ s}$ , consistent with other studies (Johnson et al., 1977). For Hb, the solution and cellular  $T_{1e}$  values are also quite similar,  $7.5 \pm 3.2 \times 10^{-12} \text{ s}$  and  $6.5 \pm 3.6 \times 10^{-12} \text{ s}$ . Despite the difference in the rotational correlation time, the cellular environment does not significantly alter the electronic structure. The spectral similarity between the solution and cellular state spectra in the proximal histidyl  $N_\delta\text{H}$  chemical shift and the heme methyl spread in the region between 30 and 10 ppm, where the peak positions are particularly sensitive to the electronic orbital ground, would also argue for a consistent electronic state in solution and in the cell (La Mar, 1979; La Mar et al., 1993; Busse and Jue, 1994).

Between Mb and Hb some difference in electronic structure may be present, given the different  $T_{1e}$  values and the contrasting  $T_1$ s of the proximal histidyl  $N_\delta\text{H}$ . But the limited accuracy of the Hb  $T_{1e}$  values currently precludes any definitive interpretation. These observations warrant further investigation.

### Separation of cellular Mb from Hb signals in vivo

Analyzing the Mb physical properties in an isolated heart establishes a critical model for exploring the Mb function in the in situ myocardium. However, in blood-perfused myocardium, the Hb signal may interfere with the Mb signal, as researchers have already noted (Kreutzer et al., 1993). The contrasting cellular Hb versus Mb  $T_2$  relaxation provides a basis for separating the Mb from the Hb signals. Fig. 5 displays clearly that a 1-ms spin echo will distinguish a 0.1 mM Mb signal in the presence of packed erythrocytes. Moreover, the severity of the erythrocyte Hb signal interference contribution depends on the vascular-to-tissue volume ratio, which in certain skeletal muscles accounts for

only 2–5%. In such cases, the Hb spectral contamination would be minimized (Kreutzer et al., 1993).

### CONCLUSION

Both the cellular Mb and Hb signals are NMR visible. Field-dependent analysis of the Mb/Hb transverse relaxation reveals a cellular rotational correlation time increase of 1.4 and 2.2 times over the corresponding values in solution. Myoglobin appears sufficiently mobile to play a central role in facilitating oxygen diffusion in the cell. The contrasting relaxation times suggest a straightforward method in discriminating the Mb from the Hb signal in blood-perfused tissue in vivo.

We gratefully acknowledge grant support from the National Institutes of Health (GM44916); a UCD Hibbard Williams grant; the American Heart Association, CA Affiliate 92-221; the National Institutes of Health (HL 09274 to YC), and the Deutsche Forschungsgemeinschaft Kr1026 (UK).

### REFERENCES

- Antonini, E., and M. Brunori. 1971. Hemoglobin and Myoglobin in Their Reactions with Ligands. Elsevier/North Holland, Amsterdam.
- Busse, S., and T. Jue. 1994. Two dimensional characterization of the deoxymyoglobin heme pocket. *Biochemistry*. 33:10934–10943.
- Chung, Y., and T. Jue. 1996. Cellular response to reperfused oxygen in postischemic myocardium. *Am. J. Physiol.* 271:H1166–H1173.
- Conley, K. E., and C. Jones. 1996. Myoglobin content and oxygen diffusion: model analysis of horse and steer muscle. *Am. J. Physiol.* 271:C2027–C2036.
- Dalvit, C., and P. E. Wright. 1987. Assignment of resonances in the  $^1\text{H}$  nuclear magnetic resonance spectrum of the carbon monoxide complex of sperm whale myoglobin by phase-sensitive two-dimensional techniques. *J. Mol. Biol.* 194:313–327.
- Everhart, C. H., D. A. Gabriel, and C. S. Johnson, Jr. 1982. Tracer diffusion coefficients of oxyhemoglobin A and oxyhemoglobin S in blood cells as determined by pulsed field gradient NMR. *Biophys. Chem.* 16:241–245.
- Everhart, C. H., and C. S. Johnson, Jr. 1982. The determination of tracer diffusion coefficients for proteins by means of pulsed field gradient NMR with applications to hemoglobin. *J. Magn. Res.* 48:466–474.
- Fetler, B. K., V. Simplaceanu, and C. Ho. 1995.  $^1\text{H}$  NMR investigation of the oxygenation of hemoglobin in intact human red blood cells. *Biophys. J.* 68:681–693.
- Gueron, M. 1975. Nuclear relaxation in macromolecules by paramagnetic ions: a novel mechanism. *J. Magn. Res.* 19:58–66.
- Ho, C., and I. Russu. 1981. Proton nuclear magnetic resonance investigation of hemoglobins. *Methods Enzymol.* 76:275–312.
- Johnson, M. E., L. W. M. Fung, and C. Ho. 1977. Magnetic field and temperature induced line broadening in the hyperfine-shifted proton resonances of myoglobin and hemoglobin. *J. Am. Chem. Soc.* 99:1245–1250.
- Jue, T., G. N. La Mar, K. Han, and Y. Yamamoto. 1984. NMR study of the exchange rates of allosterically responsive labile protons in the heme pockets of hemoglobin A. *Biophys. J.* 46:117–120.
- Jurgens, K. D., T. Peters, and G. Gros. 1994. Diffusivity of myoglobin in intact skeletal muscle cells. *Proc. Natl. Acad. Sci. USA.* 91:3829–3833.
- Kreutzer, U., Y. Chung, D. Butler, and T. Jue. 1993.  $^1\text{H}$ -NMR characterization of the human myocardium myoglobin and erythrocyte hemoglobin signals. *Biochim. Biophys. Acta.* 1161:33–37.
- Kreutzer, U., and T. Jue. 1991.  $^1\text{H}$  nuclear magnetic resonance deoxymyoglobin signal as indicator of intracellular oxygenation in myocardium. *Am. J. Physiol.* 30:H2091–H2097.

- Kreutzer, U., and T. Jue. 1995. Critical intracellular oxygen in the myocardium as determined with the  $^1\text{H}$  NMR signal of myoglobin. *Am. J. Physiol.* 268:H1675–H1681.
- Kreutzer, U., D. S. Wang, and T. Jue. 1992. Observing the  $^1\text{H}$  NMR signal of the myoglobin Val-E11 in myocardium: an index of cellular oxygenation. *Proc. Natl. Acad. Sci. USA.* 89:4731–4733.
- Kuchel, P. W., and B. E. Chapman. 1991. Translational diffusion of hemoglobin in human erythrocytes and hemolysates. *J. Magn. Res.* 94:574–580.
- La Mar, G. N. 1979. Model compounds as aids in interpreting NMR spectra of hemoproteins. In *Biological Applications of Magnetic Resonance*. R. G. Shulman, editor. Academic Press, New York. 305–343.
- La Mar, G. N., D. L. Budd, and H. Goff. 1977. Assignment of proximal histidine proton NMR peaks in myoglobin and hemoglobin. *Biochem. Biophys. Res. Commun.* 77:104–110.
- La Mar, G. N., J. D. Cutnell, and S. B. Kong. 1981. Proton magnetic resonance characterization of the dynamic stability of the heme pocket in myoglobin by the exchange behavior of the labile proton of the proximal histidyl imidazole. *Biophys. J.* 34:217–225.
- La Mar, G. N., N. L. Davis, R. D. Johnson, W. S. Smith, J. B. Hauksson, D. L. Budd, F. Dalichow, K. C. Langry, I. K. Morris, and K. M. Smith. 1993. Nuclear magnetic resonance investigation of the electronic structure of deoxymyoglobin. *J. Am. Chem. Soc.* 115:3869–3876.
- La Mar, G. N., K. Nagai, T. Jue, D. L. Budd, K. Gersonde, H. Sick, T. Kagimoto, A. Hayashi, and F. Taketa. 1980. Assignment of proximal histidyl imidazole exchangeable resonances to the individual subunits of Hb A, Boston, Iwate, and Milwaukee. *Biochim. Biophys. Acta.* 96:1172–1177.
- Livingston, D. J., G. N. La Mar, and W. D. Brown. 1983. Myoglobin diffusion in bovine heart muscle. *Science.* 220:71–73.
- London, R. E., C. T. Gregg, and N. A. Matwiyoff. 1975. Nuclear magnetic resonance of rotational mobility of mouse hemoglobin labeled with  $[2-^{13}\text{C}]$  histidine. *Science.* 188:266–268.
- Mabbutt, B. C., and P. E. Wright. 1985. Assignment of heme and distal amino acid resonances in the  $^1\text{H}$ -NMR spectra of the carbon monoxide and oxygen complexes of sperm whale myoglobin. *Biochim. Biophys. Acta.* 832:175–185.
- Marshall, A. G., K. M. Lee, and P. W. Martin. 1980. Determination of rotational correlational time from perturbed angular correlations of gamma rays: apomyoglobin reconstituted with  $^{111}\text{In}$ (III) mesoporphyrin IX<sup>1</sup>. *J. Am. Chem. Soc.* 102:1460–1462.
- Marshall, A. G., K. M. Lee, and P. W. Martin. 1983. Motional freedom of the central metal atom in apohemoglobin reconstituted with  $^{111}\text{In}$ : protoporphyrin. IX. Time-differential perturbed gamma-ray angular correlations. *J. Chem. Phys.* 78:1528–1532.
- Papadopoulos, S., K. D. Jurgens, and G. Gros. 1995. Diffusion of myoglobin in skeletal muscle cells—dependence on fibre type, contraction and temperature. *Pflugers Arch. Eur. J. Physiol.* 430:519–525.
- Phillips, S. E. 1980. Structure and refinement of oxymyoglobin at 1.6 Å resolution. *J. Mol. Biol.* 142:531–554.
- Riveros-Moreno, V., and J. B. Wittenberg. 1972. The self diffusion coefficients of myoglobin and hemoglobin in concentrated solutions. *J. Biol. Chem.* 247:895–901.
- Stryer, L. 1965. The interaction of naphthalene dye with apomyoglobin and apohemoglobin—a fluorescent probe of non-polar binding sites. *J. Mol. Biol.* 13:482–495.
- Takahashi, S., A. K.-L. C. Lin, and C. Ho. 1980. Proton nuclear magnetic studies of hemoglobin M Boston (a58E7 His→Tyr) and M Milwaukee (b67Val→Tyr): spectral assignments of hyperfine shifted proton resonances and proximal histidyl NH resonances to the a and b chains of normal human adult hemoglobin. *Biochemistry.* 19:5196–5202.
- Takano, T. 1977a. Structure of myoglobin refined at 2.0 Å resolution. II. Structure of deoxymyoglobin from sperm whale. *J. Mol. Biol.* 110:569–584.
- Takano, T. 1977b. Structure of myoglobin refined at 2.0 Å resolution I. Crystallographic refinement of metmyoglobin from sperm whale. *J. Mol. Biol.* 110:537–568.
- Vega, A. J., and D. Fiat. 1976. Nuclear relaxation processes of paramagnetic complexes. The slow-motion case. *Mol. Phys.* 31:347–355.
- Viggiano, G., N. T. Ho, and C. Ho. 1979. Proton nuclear magnetic resonance and biochemical studies of oxygenation of human adult hemoglobin in deuterium oxide. *Biochemistry.* 18:5238–5247.
- Wang, D.-J., S. Nioka, Z. Wang, J. S. Leigh, and B. Chance. 1993. NMR visibility studies of N-8 proton of proximal histidine in deoxyhemoglobin in lysed and intact red cells. *Magn. Res. Med.* 30:759–763.
- Wittenberg, B. A., and J. B. Wittenberg. 1989. Transport of oxygen in muscle. *Annu. Rev. Physiol.* 51:857–878.
- Wittenberg, J. B. 1970. Myoglobin-facilitated oxygen diffusion: role of myoglobin in oxygen entry into muscle. *Physiol. Rev.* 50:559–636.
- Yguerabide, J., H. F. Epstein, and L. Stryer. 1970. Segmental flexibility in an antibody molecule. *J. Mol. Biol.* 51:573–590.